

A summertime near-ground velocity profile of the Bora wind

Petra Lepri¹, Hrvoje Kozmar^{*2}, Željko Večenaj³ and Branko Grisogono³

¹Meteorological and Hydrological Service, Grič 3, 10000 Zagreb, Croatia

²Faculty of Mechanical Engineering and Naval Architecture, University of Zagreb,
Ivana Lučića 5, 10000 Zagreb, Croatia

³Department of Geophysics, Faculty of Science, University of Zagreb,
Horvatovac 95, 10000 Zagreb, Croatia

(Received May 30, 2014, Revised August 20, 2014, Accepted August 30, 2014)

Abstract. While effects of the atmospheric boundary layer flow on engineering infrastructure are more or less known, some local transient winds create difficulties for structures, traffic and human activities. Hence, further research is required to fully elucidate flow characteristics of some of those very unique local winds. In this study, important characteristics of observed vertical velocity profiles along the main wind direction for the gusty Bora wind blowing along the eastern Adriatic coast are presented. Commonly used empirical power-law and the logarithmic-law profiles are compared against unique 3-level high-frequency Bora measurements. The experimental data agree well with the power-law and logarithmic-law approximations. An interesting feature observed is a decrease in the power-law exponent and aerodynamic surface roughness length, and an increase in friction velocity with increasing Bora wind velocity. This indicates an urban-like velocity profile for smaller wind velocities and rural-like velocity profile for larger wind velocities, which is due to a stronger increase in absolute velocity at each of the heights observed as compared to the respective velocity gradient (difference in average velocity among two different heights). The trends observed are similar during both the day and night. The thermal stratification is near neutral due to a strong mechanical mixing. The differences in aerodynamic surface roughness length are negligible for different time averaging periods when using the median. For the friction velocity, the arithmetic mean proved to be independent of the time record length, while for the power-law exponent both the arithmetic mean and the median are not influenced by the time averaging period. Another issue is a large difference in aerodynamic surface roughness length when calculating using the arithmetic mean and the median. This indicates that the more robust median is a more suitable parameter to determine the aerodynamic surface roughness length than the arithmetic mean value. Variations in velocity profiles at the same site during different wind periods are interesting because, in the engineering community, it has been commonly accepted that the aerodynamic characteristics at a particular site remain the same during various wind regimes.

Keywords: Bora; velocity profile; aerodynamic surface roughness length; friction velocity; logarithmic-law; power-law; field measurements

1. Introduction

While the effects of the classical atmospheric boundary layer (ABL) flow on engineering

*Corresponding author, Associate Professor, E-mail: hrvoje.kozmar@fsb.hr

infrastructure, traffic and human activities are well-known, characteristics of some very unique local winds still need to be fully described. An example is the gusty Bora wind blowing along the eastern Adriatic coast, which significantly influences local wind energy yield, fatigue of wind energy structures and the agriculture and optimal functioning of transportation networks (e.g., Kozmar *et al.* 2012a,b). Previous meteorological and geophysical studies have provided background on the physics and meso-scale features of the Bora (Jurčec 1981, Smith 1987, Grubišić 2004, Grisogono and Belušić 2009); however further work is required to fully determine Bora micro-scale characteristics in a form usable for engineers.

In general, the Bora is a very strong, usually dry and always gusty wind that blows from the northeast across the coastal mountain ranges on the eastern coast of the Adriatic Sea, from Trieste to Dubrovnik and further south (e.g., Yoshino 1976, Makjanić 1978, Bajić 1988, 1989, Tutiš 1988, Vučetić 1991, Belušić and Klaić 2004, 2006). Known for its spatiotemporal variability, the Bora is more common in winter when it can last from several hours up to several days (e.g., Jurčec 1981, Poje 1992, Enger and Grisogono 1998, Jeromel *et al.* 2009). Its mean velocity, usually not less than 5, and often surpassing even 30 m/s, is less significant than its gusts that can reach velocities up to three or even five times the average (e.g., Petkovšek 1987, Belušić and Klaić 2004, 2006, Grisogono and Belušić 2009, Večenaj *et al.* 2010, Belušić *et al.* 2013). There is no precise and/or strict definition of Bora, primarily due to its extreme spatial variability along the eastern Adriatic coast (e.g., Poje 1992, Horvath *et al.* 2009, Večenaj *et al.* 2012). However, its basic characteristics mentioned above make every time series of horizontal wind recorded at the coast with azimuth from the first quadrant, blowing at least for three hours with mean wind speed ≥ 5 m/s and its standard deviation comparable to the mean, to be considered as a potential Bora event.

The synoptic situation associated with the long lasting Bora is characterized by a persistent cyclone over the Adriatic region and/or a high pressure centre over the Central Europe (e.g., Jurčec 1981, Heimann 2001, Belušić *et al.* 2013). The cyclone over the sea draws continental air from the lower troposphere across the coastal mountain ranges. Similarly, the synoptic anticyclone forces air from the Pannonia Basin and the Central Europe across mountains towards the Adriatic. The passage of a cold front across the Adriatic can also trigger a short-lasting Bora (e.g., Jurčec and Visković 1994). Shallow or deep Boras occur depending on the intensity and evolution of the cyclogenesis and its synchronization with the upper tropospheric flow (e.g., Grisogono and Belušić 2009). A shallow Bora develops if the flow remains confined in the lower atmosphere; in this case synoptic scale inversions usually play significant roles (e.g., Smith 1987).

The seminal works of Klemp and Durran (1987), and Smith (1987), showed independently that the strong Bora flow can be treated, to a very good approximation, as a nonlinear hydraulic flow, which also means a lack of significant stratification effects in the area of highest wind speeds. Namely, the resonance between the flow and underlying terrain is so strong that the wave breaking diminishes any stratification near the surface where high speeds are obtained (e.g., Grisogono and Belušić 2009). Depending on the triggering baric system, the Bora can be cyclonic, anticyclonic or frontal. The cyclonic or ‘dark’ Bora brings clouds with a high possibility for precipitation, whereas the anticyclonic or ‘clear’ Bora is related to fair weather (e.g., Jurčec and Visković 1994). Spatiotemporal statistical analysis shows that the frequency of Bora occurrence in the eastern Adriatic decreases from northwest to southeast (e.g., Poje 1992), and its strength weakens seaward from the shore in a way that it is rarely stormy in the western Adriatic (e.g., Enger and Grisogono 1998).

Bora research intensified with development of advanced measurements and numerical atmospheric models that caused a change in basic understanding of the triggering mechanism for

severe Bora. Originally, a ‘katabatic type’ perspective prevailed (e.g., Yoshino 1976, Jurčec 1981). However, a concern with this approach was that simple katabatic flows are usually not capable of producing continuous mean wind velocities of about 20 m/s, as such wind velocities require large surface potential temperature deficits. Presently, hydraulic theory of strong to severe Bora with orographic wave breaking is commonly accepted in the meso-scale dynamics community, at least for the NE Adriatic coast (Smith 1987, Enger and Grisogono 1998, Grubišić 2004, Grisogono and Belušić 2009). Downslope windstorm gusts typically exhibit a quasi-periodic behaviour (Petkovšek 1976, 1982, 1987, Rakovec 1987, Neiman *et al.* 1988), as Bora pulsations emerge in periods usually between 3 and 11 minutes (Belušić *et al.* 2004, 2006, 2007). Their origin is non-local, as their presence is not related to any local generating mechanism. The Bora has historically been more studied in the northern Adriatic, partly due to the complex orography of the central and southern Adriatic coast. In the north, the incoming flow is less influenced by the upwind mountains, and there are fewer mountain gaps, coastal valleys and significant estuaries (e.g., Grisogono and Belušić 2009, Belušić *et al.* 2013). Downslope winds with similar wind dynamics to the Croatian Bora are common in other world regions, such as Japan, Russia, Kurdistan, Iceland, Austria, Rocky Mountains in the Northern America, etc. (e.g., Jurčec 1981, Neiman *et al.* 1988, Ágústsson and Ólafsson 2007, Jackson *et al.* 2013).

In this study, detailed high-frequency measurements on a meteorological tower close to the city of Split, Croatia, on the central eastern Adriatic coast, were performed. As the Bora turbulence has been addressed only recently (Večenaj *et al.* 2010, 2012), but still insufficiently for the central Adriatic coast (Magjarević *et al.* 2011), this study attempted to assess some of the basic properties of near-surface summertime Bora turbulence. In particular, characteristics of wind velocity vertical profiles with respect to the commonly employed power-law and logarithmic-law are examined.

2. Methodology

While the approximation of the vertical profile of wind velocity by using the empirical power-law has been rarely used in the recent meteorological studies (because of the lack of explicit buoyancy effects in such formulations), it still remains pertinent in the field of wind engineering and environmental aerodynamics. This approach was originally suggested by Hellman (1916) as

$$\frac{\bar{u}_z}{\bar{u}_{\text{ref}}} = \left(\frac{z-d}{z_{\text{ref}}-d} \right)^\alpha \quad (1)$$

where \bar{u}_z represents time averaged mean wind velocity in the downwind x -direction at the height z , \bar{u}_{ref} is the corresponding time-averaged mean wind velocity at the reference height z_{ref} , d is displacement height, and α is power-law exponent dependent on local terrain roughness, atmospheric stability and the time averaging interval. Dyrbye and Hansen (1997) indicated that a power-law solution can be used to represent the velocity profiles throughout an entire depth of the ABL up to several hundreds of meters. On the other hand, within the inertial sub-layer (also called the Prandtl constant-flux layer), which can extend up to approximately 100 m height (e.g., Garratt 1992, Holmes 2007), the logarithmic-law represents well the average wind velocity profile. Unlike the power-law, which does not have a term to take into account the effects of the thermal stratification on the velocity profile, the logarithmic-law has that option included. Stull (1988) provided the logarithmic-law with the thermal stability correction ψ as

$$\frac{\bar{u}_z}{u_*} = \frac{1}{\kappa} \left[\ln \left(\frac{z-d}{z_0} \right) - \psi \left(\frac{z-d}{L} \right) \right] \quad (2)$$

Here, u_* is friction velocity (also known as shear velocity), κ is von Kármán constant with the value used here equal to 0.41 (Högström 1988, Stull 1988), z_0 is aerodynamic surface roughness length, L is Obukhov length and ψ is an empirical function of z and L . In general, for some engineering application in the lower ABL up to 100 m height, the logarithmic-law with the thermal stability correction can be more appropriate to use than the power-law. This is for example the case for air pollution dispersion and dilution problems taking place at low wind velocities, as in those situations the thermally-induced turbulence starts to dominate the mechanically-generated turbulence.

Thermal stratification is commonly described with the dimensionless parameter ζ , (also called a stability parameter, e.g., Stull, 1988) calculated using the expression

$$\zeta = \frac{z}{L} \quad (3)$$

Positive ζ implies a statically stable stratification, negative ζ implies a statically unstable stratification and ζ equal to zero implies statically neutral stratification. Since a typical Bora surface layer is almost always near a neutral stratification, as will be shown later in this study, it makes sense to proceed with such simple relations as (1) and (2) even though horizontal homogeneity is often violated for Bora flows. Typical values of terrain parameters z_0 , d and α are reported in Table 1.

Aerodynamic surface roughness length z_0 and displacement height d are reported as indicated in the international standard ESDU85020 (1985), while the power-law exponent α is calculated using the expression by Counihan (1975)

$$\alpha = 0.0961(\log z_0) + 0.016(\log z_0)^2 + 0.24 \quad (4)$$

The power-law is commonly used in wind power assessment where wind at a certain height needs to be estimated from wind observations from another height. Although the wind profile of the ABL is logarithmic near surface (e.g., Stull 1988), and is best approximated with the logarithmic wind profile that accounts for certain surface roughness and atmospheric stability, the wind power-law is often used as a substitute when surface roughness or stability information data are not available. In general, an increase in terrain urbanization results in increased values of α , z_0 , and u_* .

3. Data collection and instruments

The measurements considered in this study were carried out from April 2010 through June 2011 at the meteorological tower on the Pometeno brdo in the hinterland of Split, Croatia, which is on the lee side of the central Dinaric Alps (Fig. 1).

Table 1 Typical values of terrain parameters z_0 and d reported in ESDU85020 (1985) and α calculated from Eq. (4)

Terrain description	z_0 (m)	d (m)	α (-)
City centres	0.7	15 to 25	0.23
Forests			
Small towns			
Suburbs of large towns and cities	0.3	5 to 10	0.19
Wooded country (many trees)			
Outskirts of small towns			
Villages	0.1	0 to 2	0.16
Countryside with many hedges, some trees and some buildings			
Open level country with few trees and hedges and isolated buildings; typical farmland			
Fairly level grass plains with isolated trees	0.03	0	0.13
Very rough sea in extreme storms (once in every 50 years extreme)	0.01	0	0.11
Flat areas with short grass and no obstructions	0.003	0	0.10
Runway area of airports			
Rough sea in annual extreme storms			
Snow covered farmland	0.001	0	0.10
Flat desert or arid areas			
Inland lakes in extreme storms			



(a)



(b)

Fig. 1 (a) The geographic position of the Pometeno brdo (43°36'28.9"N, 16°28'37.4"E, 618 m ASL), Croatia. The Adriatic sea is to the west and south. Lower left corner the geographic position of Croatia in Europe. (b) Anemometer setup on the meteorological tower at the Pometeno brdo (from Magjarević 2011), the sensors used in this study are indicated (two circles and a working man)

The exact geographical coordinates of the measurement site are $43^{\circ}36'28.9''\text{N}$ and $16^{\circ}28'37.4''\text{E}$ with the highest peak 618 m above the mean sea level. Three velocity components (east, north and vertical) and ultrasonic temperature were measured using Windmaster Pro ultrasonic anemometers (Gill Instruments) with the sampling frequency of 5 Hz. Anemometers were mounted on a 60 m high meteorological tower at three height levels, i.e., at 10, 20 and 40 m. As the height difference between the highest and the lowest measuring points is fairly small, i.e., 30 m, in this study it is considered that in this near-surface range the wind direction does not change significantly with height due to an intense mixing of the flow (the average wind direction change through those 30 m is about $\pm 5^{\circ}$). However, the angle between the near-surface and geostrophic wind far away from the ground can reach as high as 35° (e.g., Grisogono 2011) due to the Coriolis force and other effects that need to be taken into account for measurements at heights significantly greater than the one used in this study. Moreover, three measuring heights are considered to be sufficient to capture near-ground velocity profiles with satisfactory accuracy, whereas the main scope of this work is to determine trends in changing power-law coefficient, friction velocity, and aerodynamic surface roughness length profiles with regard to the mean wind velocity rather than to attempt to improve fitting methodology. Additionally, typical meteorological surface layer measurements for nearly neutral static (i.e., thermal) stability conditions usually comprise only one or two levels (e.g., Stull 1988, Likso and Pandžić 2011). Each anemometer was mounted on one end of the 2 m long aluminium boom, whose other end was fixed to the tower so that the anemometers were facing the main Bora wind direction. In this way, the influence of the tower on measurements of the Bora flows was avoided. Anemometers were connected to a Campbell Scientific data logger CR1000 and the whole system was solar powered.

An isolated summer Bora event, which lasted from 24 to 27 July 2010 in total duration of 62 hours (Magjarević *et al.* 2011), is considered in this study. In this episode the wind was relatively strong and long lasting, with mean hourly velocities larger than 15 m/s.

Due to the potential applicability of the power- and logarithmic-law for Bora wind profiles, a suitable coordinate system is the one with the x -axis aligned along the mean wind direction. As the mean wind direction at 10 m height is $\approx 54^{\circ}$, at 20 m it is $\approx 51^{\circ}$ and at 40 m it is $\approx 43^{\circ}$, linearly interpolated mean wind direction at 25 m height (the centre between 10 m and 40 m) is 49° (Večenaj 2012). Therefore, the original data for the two horizontal velocity components are rotated for 221° counter clockwise. Fig. 2 shows the original data for all three velocity components in the new coordinate system with x -axis aligned along the mean Bora direction.

For the calculation of time averaged wind velocity, the moving average is used. To test the sensitivity of results to the choice of the length of the moving average, moving averages with different averaging periods are applied. For this Bora episode, there are strong indications that quasi-periodic pulsations occur at the period of about 8 min (Belušić *et al.* 2007, Horvath *et al.* 2012, Večenaj 2012). Also, Magjarević *et al.* (2011) used methodology from Večenaj *et al.* (2012) and found that the period of 17 min represents a suitable turbulence averaging scale (scale which separates turbulence at small scales from the mean flows at large scales) for this Bora episode. Therefore, scales of 8 and 17 min arise as the natural choice for the above mentioned test. In addition to these two dynamically relevant scales, one shorter (5 min) and one longer (20 min) scales are included to encompass the most relevant Bora related scales.

The choice for the shorter averaging scale is motivated by Belušić *et al.* (2006, 2007), who found that Bora pulsations, i.e. quasi-periodic contribution to the total wind gustiness, might occur at periods roughly between 3 and 11 min. On the other hand, the choice for the longer averaging scale is motivated by Magjarević *et al.* (2011), who found that the uncertainty for their 17-min

scale amounts ± 3 min. While there is some arbitrariness in the choice of these two additional scales, the important point is that they encompass the two dynamically relevant scales. The obtained data, which for certain moving average in x -direction consisted of three time series of time averaged wind velocities (one time series for each height), each having more than 10^6 data points, were then used to verify the applicability of the power- and logarithmic-law to the Bora wind.

Time averaged mean wind velocities in x -direction at three levels were then scaled with time averaged mean wind velocity in x -direction at 40 m height, and the power-law exponent α was calculated using a scaled data adjustment to the power-law given in Eq. (1). Since the measuring site is mostly rocky without any significant vegetation, the displacement height d can be taken to be zero, as indicated in Table 1. For each time step, there were three data points, one at each height level, and the power-law coefficient was calculated as the best fit to the power-law for these three data points. Scaling for the two other levels is not shown because the results are basically the same.

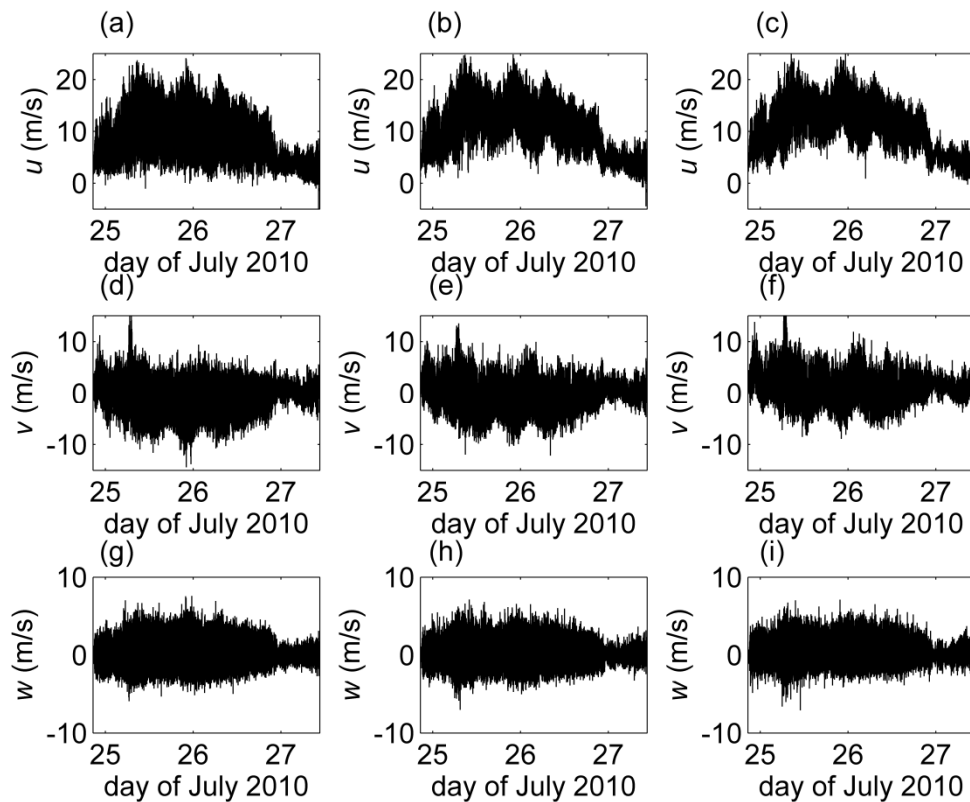


Fig. 2 Original data at 10 m height (left), 20 m (middle) and 40 m (right) at the Pometeno brdo tower; longitudinal (u), lateral (v) and vertical (w) velocity components recorded from July 24 to 27, 2010 shown in the coordinate system with x -axis aligned along the mean Bora direction

To test whether the logarithmic-law is applicable to the Bora wind, u_* and z_0 were calculated in two ways, the first by data adjustment to the logarithmic-law, and the second by directly applying the logarithmic-law to a layer between 10 and 40 m with the value of d here also equal to zero. The friction velocity can then be calculated from the expression

$$u_* = \frac{\kappa(\bar{u}_2 - \bar{u}_1)}{\ln\left(\frac{z_2}{z_1}\right)} \quad (5)$$

where \bar{u}_1 and \bar{u}_2 represent time averaged mean wind velocities in x-direction at 10 m and 40 m, respectively. Aerodynamic surface roughness length is given by

$$z_0 = z_1 \exp\left(-\frac{\bar{u}_1}{\bar{u}_2 - \bar{u}_1} \ln \frac{z_2}{z_1}\right) \quad (6)$$

As in the power-law adjustment verification, the adjustment to the logarithmic-law is performed on three data points measured at the same time at different height levels in each step of the calculation. Using the linear regression method, a straight line was fitted to the particular three points and from the obtained parameters the corresponding values of u_* and z_0 were calculated.

4. Results and discussion

In this section applicability of the empirical power-law and the logarithmic-law on the Bora wind velocity profiles is investigated, as well as velocity profile characteristics during the wind gusts and the lower wind velocity periods. In Tables 2-6 statistical parameters α , u_* , and z_0 are presented for averaging periods from 5 min to 20 min.

In all tests, the arithmetic mean value for α is 0.169 indicating its robustness in regard to the data averaging periods deployed. This value is in agreement with the median 0.162 that reflects the normal-like distribution of the power-law exponent α for different averaging periods. Since field measurements can last several days and longer, as is the case in this study, the measured data sometimes drift with time mostly because of natural variations in background flow. Hence, for those studies the median may be a more suitable parameter than the arithmetic mean to correctly describe the dominant values. That is also why for longer averaging periods the range between the minimal and maximal α values decreases. On the other hand, in wind-tunnel experiments the time records usually do not exceed several minutes and this often results in data being scattered normally around nearly constant values.

The standard deviation, which defines data variations from the average or expected value (e.g., Wilks 1995), with observed values between 0.046 and 0.059, indicates that the data moderately (around 20%) differs from the average value. The value of the coefficient of determination, r^2 , which indicates a goodness of the power-law fit to the measured data, slightly changes for different averaging periods. In particular, r^2 ranges from 0.902 to 0.919 indicating that the power-law applies well to the Bora surface layer wind velocity profile. The estimated mean α being around 0.17 is close to ESDU85020 (1985) values reported for outskirts of small towns, villages, countryside with many hedges, some trees and some buildings (Table 1). A summary of the

statistics for the u_* and z_0 dependence on the averaging period from 5 to 20 min is given in Tables 3-6.

Table 2 Summary statistics for the power-law exponent α for different averaging periods, r^2 is the coefficient of determination

Statistical parameters	Averaging period			
	5 minutes	8 minutes	17 minutes	20 minutes
Median (-)	0.163	0.163	0.162	0.162
Arithmetic mean (-)	0.169	0.169	0.169	0.169
Min. value (-)	0.000	0.004	0.063	0.069
Max. value (-)	0.436	0.383	0.364	0.351
Standard deviation (-)	0.059	0.053	0.047	0.046
r^2 (-)	0.902	0.909	0.918	0.919

Table 3 Summary statistics for Bora friction velocity u_* for different averaging periods obtained by the logarithmic-law adjustment

Statistical parameters	Averaging period			
	5 min	8 min	17 min	20 min
Median (m/s)	0.696	0.704	0.713	0.716
Arithmetic mean (m/s)	0.684	0.684	0.685	0.686
Min. value (m/s)	0.000	0.005	0.070	0.089
Max. value (m/s)	1.826	1.739	1.568	1.536
Standard deviation (m/s)	0.318	0.306	0.292	0.289
r^2 (-)	0.910	0.917	0.927	0.929

Table 4 Summary statistics for Bora friction velocity u_* for different averaging periods obtained from Eq. (5)

Statistical parameters	Averaging period			
	5 min	8 min	17 min	20 min
Median (m/s)	0.696	0.704	0.713	0.716
Arithmetic mean (m/s)	0.684	0.684	0.685	0.686
Min. value (m/s)	0.000	0.005	0.070	0.089
Max. value (m/s)	1.826	1.739	1.568	1.536
Standard deviation (m/s)	0.318	0.306	0.292	0.289

As reported in Tables 3 and 4, average u_* calculated using the data adjustment to the logarithmic-law and by applying Eq. (5) are nearly identical and not dependent on the averaging period, which is most probably due to weak, near neutral, thermal stratification of the lower troposphere during significant Bora episodes (e.g., Smith 1987, Grisogono and Belušić 2009). In particular, in all tests the arithmetic mean value for u_* calculated both ways is between 0.68 and 0.69 m/s. Therefore, similarly to the power-law exponent, u_* can be considered as robust with respect to the averaging period changes as well. The median u_* values around 0.70 m/s agree well with the u_* arithmetic mean indicating the normal-like distribution of the recorded data. As expected, the range between the minimum and maximum u_* values decreases for longer averaging periods. The standard deviation for u_* calculated both ways is between 0.289 m/s and 0.318 m/s (Tables 3 and 4) suggesting a notable, but still acceptable, spread of u_* values from their mean.

Table 5 Summary statistics for Bora aerodynamic surface roughness length z_0 for different averaging periods obtained by the logarithmic-law adjustment

Statistical parameters	Averaging period			
	5 min	8 min	17 min	20 min
Median (m)	0.038	0.038	0.037	0.037
Arithmetic mean (m)	0.113	0.103	0.092	0.090
Min. value (m)	0.000	0.000	0.000	0.000
Max. value (m)	1.680	1.400	1.218	1.045
Standard deviation (m)	0.180	0.158	0.135	0.130
r^2 (-)	0.910	0.917	0.927	0.929

Table 6 Summary statistics for Bora aerodynamic surface roughness length z_0 for different averaging periods obtained from Eq. (6)

Statistical parameters	Averaging period			
	5 min	8 min	17 min	20 min
Median (m)	0.042	0.041	0.041	0.041
Arithmetic mean (m)	0.119	0.109	0.097	0.095
Min. value (m)	0.000	0.000	0.000	0.000
Max. value (m)	1.890	1.381	1.212	1.044
Standard deviation (m)	0.190	0.163	0.139	0.134

While α and u_* appear to be independent of the averaging period, slight differences are noticed for z_0 . In particular, the average z_0 is from 0.090 m to 0.113 m when using the logarithmic-law adjustment and from 0.095 m to 0.119 m when calculating using Eq. (6) (Tables 5 and 6). A rather high standard deviation between 0.130 m and 0.190 m indicates high data dispersion, but a large r^2 between 0.910 and 0.929 still indicates that the logarithmic-law describes the data satisfactory. In addition, the observed arithmetic mean values for z_0 are roughly double the median values indicating a data distribution which is far from being normal (i.e., non-Gaussian). This indicates that the more robust median, which remains nearly the same for all averaging periods, is a more suitable parameter to determine the aerodynamic surface roughness length than the arithmetic mean value. Therefore, to visualize the data distribution during the 62 hours of measurements, the recorded number of samples for α , \bar{u} , u_* and z_0 is reported in Fig. 3. As the trends observed are nearly the same for all averaging periods investigated in this study, results are reported for the averaging time 17 min only. In addition, trends observed for u_* and z_0 are nearly the same for two procedures applied, i.e. logarithmic-law adjustment and calculation using Eqs. (5) and (6).

The reported results show nearly normal distribution for α and u_* , three-modal distribution for \bar{u} and the Poisson-like distribution for z_0 . Moreover, further analysis of synoptic charts recorded during the measurement indicates that the first peak around 5 m/s corresponds to the ending of the analysed Bora episode with dying-out of the pressure gradient and respective wind. Two other peaks in range from 11 m/s to 15 m/s are due to strong Bora pulsations with intermittent switching between gusts and weaker Bora periods.

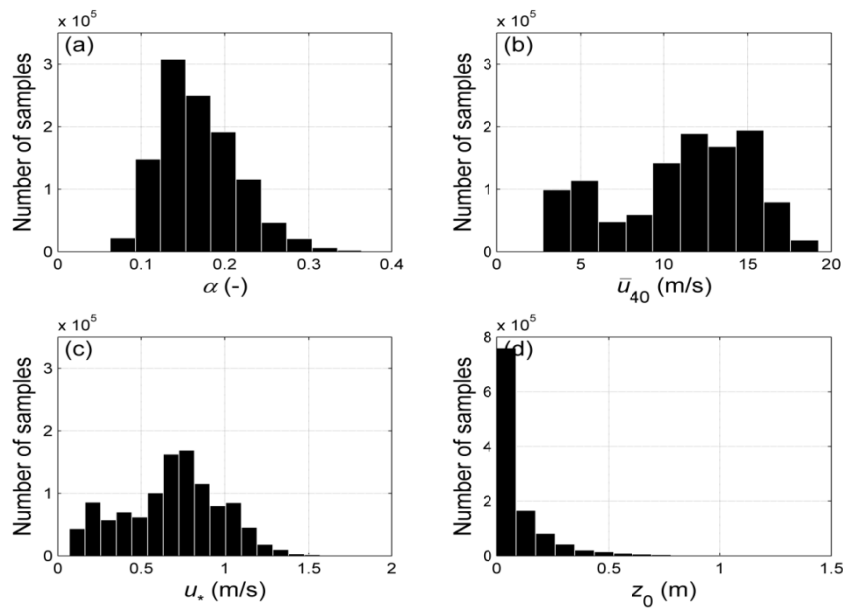


Fig. 3 A recorded number of samples for (a) α , (b) \bar{u} , (c) u_* and (d) z_0 during the measurement period

In general, the results show that both the logarithmic-law and the power-law fit the Bora wind velocity profiles very well, particularly for longer averaging periods. In addition, for this particular Bora episode, the logarithmic-law and the power-law fit the measured data better when performing the analysis by using the median rather than using the arithmetic mean wind velocity due to drifting of z_0 values during the recording time, as reported in Fig. 4.

The obtained values for z_0 are in the ESDU85020 (1985) range given for outskirts of small towns, villages and countryside with many hedges, some trees and some buildings, whereas smaller medians in comparison to arithmetic mean values indicate slightly more rural terrain exposure, as given in Table 1.

In order to investigate the dependence of α , u_* and z_0 on the average wind velocity \bar{u} , the obtained time series of those four quantities for the averaging period of 17 min are presented in Fig. 5. Time series for other three averaging periods are similar and are therefore not presented.

This graphical presentation confirms the feature already determined by using statistical methods (Tables 2-6); the Bora u_* values obtained by applying the logarithmic-law adjustment and from Eq. (5) are nearly the same for all averaging periods used, while z_0 calculated using the logarithmic-law fitting differs slightly from the results obtained using Eq. (6). A new interesting property observed, however, is a decrease in the power-law exponent and aerodynamic surface roughness length and an increase in friction velocity with increasing Bora wind velocity. This indicates an urban-like velocity profile for smaller wind velocities and rural-like velocity profile for larger wind velocities recorded during Bora gusts. Simultaneously with the local minima of the time averaged Bora mean wind velocity, the corresponding α and z_0 reach their local maxima, while the corresponding u_* reaches its local minima and vice versa. Similar trends occur both during the day and night.

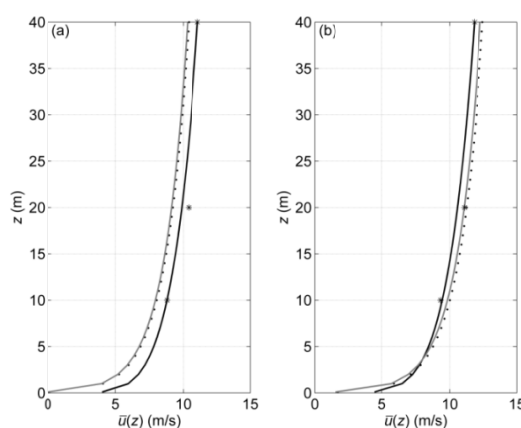


Fig. 4 Vertical velocity profile of the Bora wind; comparison of results measured at the meteorological tower with the empirical logarithmic- and power-law (a) comparison based on calculation using the arithmetic mean value, (b) comparison based on calculation using the median value. Legend: star – measured median/arithmetic mean value during 62 hours of measurement, black solid line – power-law, black dotted line – logarithmic-law, grey line – adjustment using Eqs. (5) and (6)

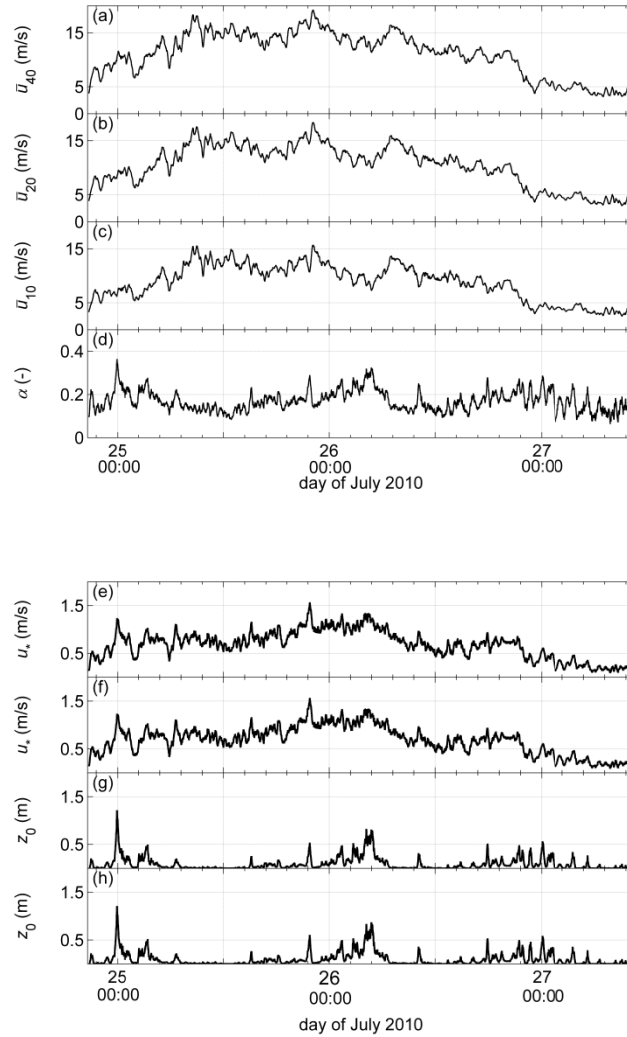


Fig. 5 Mean wind velocity averaged over the time scale of 17 min at (a) 40 m, (b) 20 m and (c) 10 m height; (d) power-law exponent α ; (e) friction velocity u_* obtained using Eq. (5); (f) friction velocity u_* calculated using the logarithmic-law adjustment; (g) aerodynamic surface roughness length z_0 calculated from Eq. (6); (h) aerodynamic surface roughness length z_0 obtained using the logarithmic-law

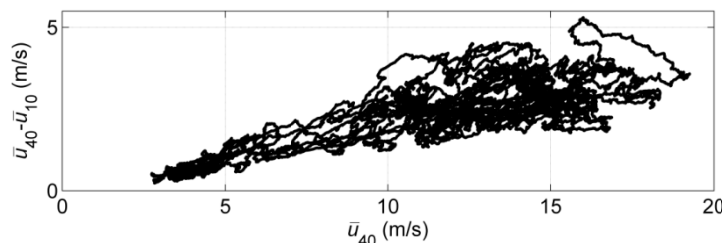


Fig. 6 The difference between time averaged mean wind velocity in the downwind x -direction at the height 40 m and 10 m against time averaged mean wind velocity in the downwind x -direction at the height 40 m

To further investigate the trends observed in Fig. 5, the relationship between a) the difference in time averaged mean wind velocities in the downwind x -direction recorded at 40 m and 10 m against b) absolute time averaged mean wind velocity in the downwind x -direction at 40 m is shown in Fig. 6. The results show that the difference between the time averaged mean wind velocities at 40 m and 10 m increases slower than the absolute magnitude of time averaged mean wind velocity in the downwind x -direction at 10 m and 40 m, which can be clearly observed in Fig. 6. Direct application of this trend to Eqs. (1), (5) and (6) yields the observation reported in Fig. 5, i.e. a decrease of α and z_0 as well as an increase of u_* with increasing wind velocity.

To investigate a possible influence of thermal stratification on the observed behaviour of α , u_* , and z_0 , the thermal stability parameter was calculated and presented in Fig. 7 along with the fitted normal distribution. The Obukhov length was calculated using the constant mean measured ultrasonic temperature; the turbulent heat flux was computed using this temperature. The same calculations were carried out using the non-constant mean ultrasonic temperature, but since those results were nearly the same as the results reported in Fig. 7, they are not presented here. Since these values are all close to zero, they clearly indicate that the observed Bora episode is near to a neutral thermal stratification.

Possible effects of the thermal stratification on Bora velocity profiles are investigated with respect to day and night as well. The time history of the stability parameter at all three heights is reported in Fig. 8.

The experimental results clearly show a moderate variation of the stability parameter during the day between 0700 and 1900 LST indicating thermally-induced atmospheric motions, while those variations are rather weak during the night along with the stability parameter close to zero. This is due to solar heating of the ground surface during the day and corresponding thermally-induced turbulence. During the night the temperature of the ground and near-ground airflows are nearly the same with a dominant mechanically-induced turbulence and stability parameter close to zero. At the end of the observed Bora episode, where smaller wind velocities were recorded, the atmosphere is thermally unstable with negative ζ values, as the thermal effects become more pronounced. It is important to note there is no correlation between those day-to-night trends in the atmospheric stability (Figs. 8(b)-8(d)) and the trend in the mean wind velocity (Fig. 8(a)). This further confirms that the atmospheric thermal stratification has no considerable influence on the observed power-law exponent, friction velocity and aerodynamic surface roughness length trends.

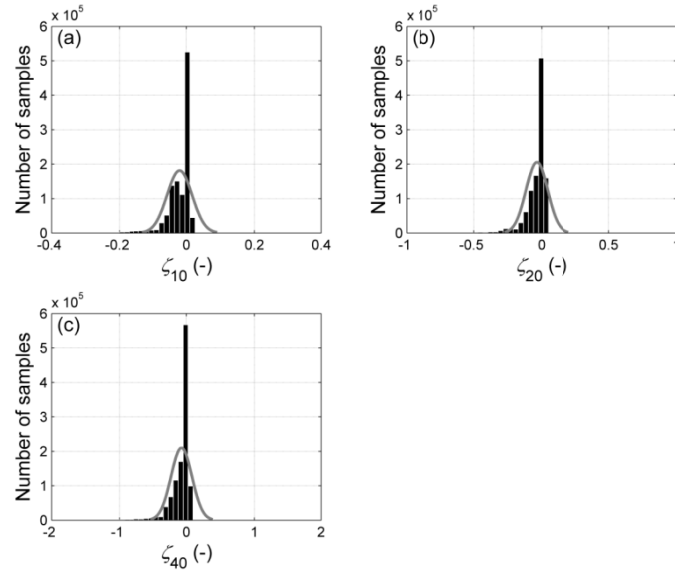


Fig. 7 A recorded number of samples for stability parameter with fitted normal distribution at (a) 10 m, (b) 20 m and (c) 40 m height

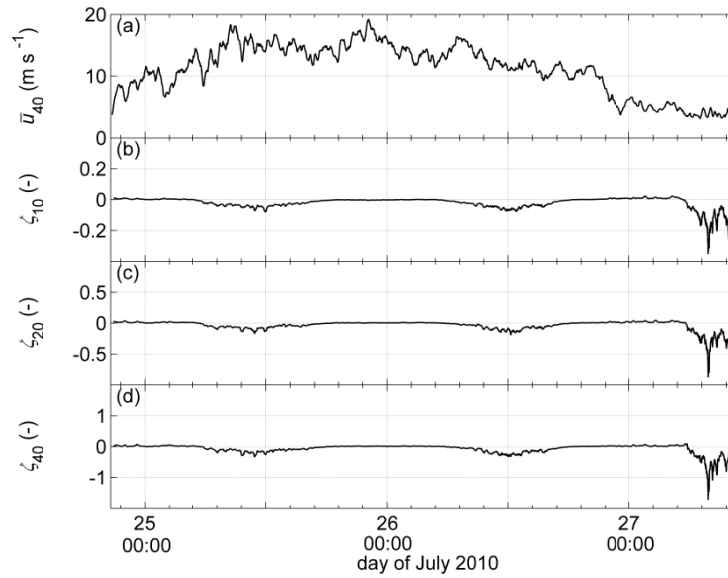


Fig. 8 (a) Mean wind velocity averaged over the time scale of 17 min at 40 m, (b) stability parameters at 10 m, (c) 20 m and (d) 40 m height

It needs to be mentioned that the trends observed apply to measurements at a specific site only. It is thought that large fractions of variability in α , u_* and z_0 are due to the intrinsic unsteadiness of the Bora at a few meso- and sub-meso scales (Belušić *et al.* 2007, Grisogono and Belušić 2009, Večenaj *et al.* 2012). However, it remains intriguing that this summertime 3-day Bora episode spreads through two broad categories of the terrain description of ESDU85020 (1985), having relatively larger α and/or relatively smaller mean z_0 than perhaps anticipated in the engineering communities. Future work is required to fully investigate the behaviour of α , u_* and z_0 in other locations, different thermal stability conditions and seasons, as well as for different height ranges of measurement points. Another research avenue shall consider Bora wind-tunnel experiments.

5. Conclusions

A summertime vertical profile of velocity was investigated for the gusty and sometimes transient Bora wind blowing along the eastern Adriatic coast. A performance of the power-law and the logarithmic-law is compared against the 3-level velocity measurements carried out at 10 m, 20 m and 40 m height on the meteorological tower near the city of Split, Croatia.

Trends in the power-law exponent α , friction velocity u_* and aerodynamic surface roughness length z_0 were studied dependent on the Bora average wind velocity. It is established, for the first time, that the observed profiles of the average wind velocity along the dominant Bora wind direction agree well with the power-law and logarithmic-law approximations. In addition, the logarithmic-law and the power-law fit the measured data better when performing the analysis by using the median rather than using the arithmetic mean wind velocity due to a drifting of mean z_0 values during the recording time.

An interesting feature is a decrease in α and z_0 and an increase in u_* with increasing Bora mean wind velocity, and vice versa. This indicates an urban-like velocity profile for smaller wind velocities and rural-like velocity profile for larger wind velocities, which is due to a stronger increase in absolute velocity at each of the heights observed as compared to the respective velocity gradient (difference in average velocity among two different heights). The trends observed are similar both during the day and night.

The thermal stratification is near neutral due to strong mechanical mixing. The differences in z_0 are negligible for different time averaging periods when using the median; for u_* the arithmetic mean proved to be independent of the time record length, while for α both the arithmetic mean and the median are not influenced by the time averaging period. Another important issue is a large difference in z_0 when calculating using the arithmetic mean and the median. This indicates that the more robust median is a more suitable parameter to determine the aerodynamic surface roughness length than the arithmetic mean value.

Variations in velocity profiles at the same site during different wind periods are interesting because in the engineering community it has been commonly accepted that the aerodynamic characteristics at a particular site remain the same during various wind regimes. While the trends observed in this study apply on measurements at a specific site, future work is required to investigate Bora turbulence characteristics at other locations, during potentially different thermal stability conditions, seasons, and for different elevations of measurement points.

Acknowledgments

Temple R. Lee and Nevio Babić are acknowledged for their reading of the final manuscript including certain scientific points. PL acknowledges the Meteorological and Hydrological Service of Croatia for support, HK is supported by the University of Zagreb grant No. 05206-2, ŽV and BG are supported by BORA, No. 119-1193086-1311 and CATURBO, No. 09/151, financed by the Croatian Ministry and National Science Foundation, respectively.

References

- Ágústsson, H. and Ólafsson, H. (2007), "Simulating a severe windstorm in complex terrain", *Meteorol. Z.*, **16**(1), 111-122.
- Bajić, A. (1988), "The strongest Bora event during ALPEX SOP", *Rasprave-Papers*, **23**(23), 1-9.
- Bajić, A. (1989), "Severe Bora on the northern Adriatic. Part I: Statistical analysis", *Rasprave-Papers*, **24**(24), 1-9.
- Belušić, D. and Klaić, Z.B. (2004), "Estimation of Bora wind gusts using a limited area model", *Tellus*, **56**, 296-307.
- Belušić, D., Pasarić, M. and Orlić, M. (2004), "Quasi-periodic bora gusts related to the structure of the troposphere", *Q. J. Roy. Meteor. Soc.*, **130**(598), 1103-1121.
- Belušić, D., Pasarić, M., Pasarić, Z., Orlić, M. and Grisogono, B. (2006), "A note on local and non-local properties of turbulence in the bora flow", *Meteorol. Z.*, **15**(3), 301-306.
- Belušić, D. and Klaić, Z.B. (2006), "Mesoscale dynamics, structure and predictability of a severe Adriatic Bora case", *Meteorol. Z.*, **15**(2), 157-168.
- Belušić, D., Žagar, M. and Grisogono, B. (2007), "Numerical simulation of pulsations in the Bora wind", *Q. J. Roy. Meteor. Soc.*, **133**(627), 1371-1388.
- Belušić, D., Hrastinski, M., Večenaj, Ž. and Grisogono, B. (2013), "Wind regimes associated with a mountain gap at the northeastern Adriatic coast", *J. Appl. Meteorol. Clim.*, **52**(9), 2089-2105.
- Counihan, J. (1975), "Adiabatic atmospheric boundary layers: a review and analysis of data from the period 1880-1972", *Atmos. Environ.*, **9**(10), 871-905.
- Dyrbye, C. and Hansen, S. (1997), *Wind Loads on Structures*, Wiley, New York, NY, USA.
- Enger, L. and Grisogono, B. (1998), "The response of bora-type flow to sea surface temperature", *Q. J. Roy. Meteor. Soc.*, **124**(548), 1227-1244.
- ESDU Data Item No. 85020 (1985), *Characteristics of Atmospheric Turbulence near the Ground*, Eng Sci Data Unit, London, UK.
- Garratt, J.R. (1992), *The Atmospheric Boundary Layer*, Cambridge University Press, New York, NY, USA.
- Grisogono, B. and Belušić, D. (2009), "A review of recent advances in understanding the meso- and micro-scale properties of the severe Bora wind", *Tellus*, **61**, 1-16.
- Grisogono, B. (2011), "The angle of the near-surface wind-turning in weakly stable boundary layers", *Q. J. Roy. Meteor. Soc.*, **137**(656), 700-708.
- Grubišić, V. (2004), "Bora-driven potential vorticity banners over the Adriatic", *Q. J. Roy. Meteor. Soc.*, **130**(602), 2571-2603.
- Heimann, D. (2001), "A model-based wind climatology of the eastern Adriatic coast", *Meteorol. Z.*, **10**(1), 5-16.
- Hellman, G. (1916), "Über die Bewegung der Luft in den untersten Schichten der Atmosphäre", *Meteorol. Z.*, **34**, 273-285.
- Holmes, J.D. (2007), *Wind Loading of Structures*, 2nd Ed., Taylor & Francis, London, UK.
- Horvath, K., Ivatek-Šahdan, S., Ivančan-Picek, B. and Grubišić, V. (2009), "Evolution and structure of severe cyclonic Bora: contrast between the northern and southern Adriatic", *Weather Forecast.*, **24**, 946-964.

- Horvath, K., Večenaj, Ž. and Grisogono, B. (2012), "Bora flow over the complex orography of the mid-Adriatic region", *Proceedings of the 15th Conference on Mountain Meteorology*, Steamboat Springs, Colorado, USA, August 2012.
- Högström, U. (1988), "Non-dimensional wind and temperature profiles in the atmospheric surface layer, a re-evaluation", *Bound. - Lay. Meteorol.*, **42**, 55-78.
- Jackson, P.L., Mayr, G. and Vosper, S. (2013), *Dynamically-Driven Winds*, (Eds., F.K. Chow, S.F.J., De Wekker and B.J. Snyder), Mountain Weather Research and Forecasting. Recent Progress and Current Challenges, Springer, Dordrecht, Netherlands.
- Jerome, M., Malačić, V. and Rakovec, J. (2009), "Weibull distribution of Bora and sirocco winds in the northern Adriatic Sea", *Geofizika*, **26**(1), 85-100.
- Jurčec, V. (1981), "On mesoscale characteristics of Bora conditions in Yugoslavia", *Pure Appl. Geophys.*, **119**, 640-657.
- Jurčec, V. and Visković, S. (1994), "Mesoscale characteristics of southern Adriatic Bora storms", *Geofizika*, **11**(1), 33-46.
- Klemp, J.B. and Durran, D.R. (1987), "Numerical modelling of Bora winds", *Meteorol. Atmos. Phys.*, **36**(1-4), 215-227.
- Kozmar, H., Butler, K. and Kareem, A. (2012a), "Transient cross-wind aerodynamic loads on a generic vehicle due to bora gusts", *J. Wind Eng. Ind. Aerod.*, **111**, 73-84.
- Kozmar, H., Procino, L., Borsani, A. and Bartoli, G. (2012b), "Sheltering efficiency of wind barriers on bridges", *J. Wind Eng. Ind. Aerod.*, **107-108**, 274-284.
- Likso, T. and Pandžić, K. (2011), "Determination of surface layer parameters at the edge of a suburban area", *Theor. Appl. Climatol.*, **108**(3-4), 373-384.
- Magjarević, V., Večenaj, Ž., Horvath, K. and Grisogono, B. (2011), "Turbulence averaging interval for summer Bora flows at the middle of the NE Adriatic coast", *Proceedings of the 31st International Conference on Alpine Meteorology*, Aviemore, Scotland, May 2011.
- Makjanić, B. (1978), "Bura, jugo, etezija", *Prilozi poznavanju vremena i klime SFRJ*, **5**, 1-43.
- Neiman, P.J., Hardesty, R.M., Shapiro, M.A. and Cupp, R.E. (1988), "Doppler lidar observations of a downslope windstorm", *Mon. Weather Rev.*, **116**(11), 2265-2275.
- Petkovšek, Z. (1976), "Periodicity of Bora gusts", *Rasprave-Papers*, **20**, 67-75.
- Petkovšek, Z. (1982), "Gravity waves and Bora gusts", *Ann. Meteor.*, **19**, 108-110.
- Petkovšek, Z. (1987), "Main Bora gusts - a model explanation", *Geofizika*, **4**, 41-50.
- Poje, D. (1992), "Wind persistence in Croatia", *Int. J. Climatol.*, **12**, 569-586.
- Rakovec, J. (1987), "Preliminary report on spectral characteristics of Bora on the island of Rab", *Geofizika*, **4**, 35-40.
- Smith, R.B. (1987), "Aerial observations of Yugoslavian Bora", *J. Atmos. Sci.*, **44**(2), 269-297.
- Stull, R.B. (1988), *An Introduction to Boundary Layer Meteorology*, Kluwer, Dordrecht, Netherlands.
- Tutiš, V. (1988), "Bora on the Adriatic coast during ALPEX SOP on 27-30 April 1982", *Rasprave-Papers*, **23**, 45-56.
- Večenaj, Ž., Belušić, D. and Grisogono, B. (2010), "Characteristics of the near-surface turbulence during a bora event", *Ann. Geophys.*, **28**, 155-163.
- Večenaj, Ž. (2012), *Characteristics of the Bora related turbulence*, Ph.D. Dissertation, University of Zagreb, Zagreb, Croatia.
- Večenaj, Ž., Belušić, D., Grubišić, V. and Grisogono, B. (2012), "Along-coast features of bora related turbulence", *Bound. - Lay. Meteorol.*, **143**(3), 527-545.
- Vučetić, V. (1991), "Statistical analysis of severe Adriatic Bora", *Cro. Met. J.*, **26**(26), 41-51.
- Wilks, D.S. (1995), *Statistical Methods in the Atmospheric Sciences*, Academic Press, New York, NY, USA.
- Yoshino, M.M. (1976), *Local Wind Bora*, University of Tokyo Press, Tokyo, Japan.